Polymerization of Silicates in Layered Double Hydroxides

Corinne Depège,[†] Fatima-Zahrae El Metoui,[†] Claude Forano,*[,†] André de Roy,[†] Jacques Dupuis,[‡] and Jean-Pierre Besse[†]

Laboratoire de Physico-Chimie des Matériaux, URA CNRS 444, and LASMEA, URA CNRS 1793, Université Blaise Pascal, Avenue des Landais, 63177 Aubière Cedex, France

Received November 9, 1995. Revised Manuscript Received January 19, 1996[⊗]

Layered double hydroxides containing silicate anions have been prepared using either a coprecipitation method or an anionic exchange reaction. The polymerization of the intercalated anions under moderate thermal treatment has been studied by PXRD, FTIR, and solid-state NMR. Grafting processes and layer condensation have been obtained leading to the preparation of new nanocomposite materials with improved physicochemical properties.

Introduction

The class of materials discussed in this paper are the layered double hydroxides (LDHs), resembling the naturally occurring hydrotalcites.[1] These can be represented by the formulas $[M^{II}_{1-x}M^{III}_{x}(OH)_2]^{x+}$-$[A^{m-}_{x/m}\cdot nH_2O]^{x-}$, where M^{II} and M^{III} represent metallic cations such as Mg^{2+}, Zn^{2+}, Cu^{2+}, Ni^{2+} and Al^{3+}, Cr^{3+}, Fe^{3+}, respectively.[2] To avoid the repetition of such heavy formulas, we shall use an abbreviated notation $[M^{II}-M^{III}-A]$.

Structurally, these compounds can be described as positively charged layers of $M(OH)_6$ edge-sharing octahedra, with the interlamellar space being occupied by neutralizing A^{m-} anions and water. One of the most important property of LDHs is that these interlamellar species can be readily ion exchanged. Various inorganic and organic anions have been intercalated in LDHs, so that much is known about their properties[3−6] and notably the pillaring of these materials by polyanions which was reported by Drezdzon[7] or Clearfield.[8]

These materials find applications mainly in heterogeneous catalysis,[9] but promising developments are expected for electrochemical analysis,[10] electrocatalysis, solid-state electrolyte materials[11] and separation processes.[12] This wide range of applications arises from both an easily controlled chemical composition of the layer and interlayer domains and a bidimensional open framework characterized by nonselective anionic exchange and intercalation properties.

Indeed, this open structure can accommodate a wide variety of interlamellar species whose chemical stability in the interlayer space depends on tight interactions either with the hydroxylated sheets or with other solvated anions. The physicochemical properties and the reactivity of the LDHs are determined not only by the chemical nature of the overall structure but also largely by these tight interactions between the host matrix and the guest species. Postsynthesis modifications of a LDH-containing reactive species can lead to a strengthening of these interactions, and significant improvement of chemical and structural stabilities can be obtained.

We have studied the reactivity of silicate anions inside the interlamellar domains of [Zn−Al] and [Zn−Cr] LDHs under moderate thermal treatment. Pillaring, grafting, and polycondensation processes are evidenced by structural and spectroscopic data. These results are compared to the chloride LDH compounds, as reference materials.

Experimental Section

Materials. For all preparations, metal chlorides or nitrates (Prolabo), sodium metasilicate, and sodium hydroxide (Fluka) were of analytical grade. All the preparative procedures were performed with deionized water under a nitrogen atmosphere to minimize the competitive intercalation of carbonate anions in LDHs.

Instruments. Powder X-ray diffraction (PXRD) patterns were obtained with a Siemens D501 X-ray diffractometer using Cu Kα radiation and fitted with a graphite backend monochromator. Fourier-transform infrared (FTIR) spectra were recorded on a Perkin-Elmer 16PC spectrophotometer on pressed KBr pellets. Thermogravimetric analyses (TGA) were performed with a Setaram TG-DTA92 thermogravimetric analyzer at a typical rate of 5 °C/min under air atmosphere. Chemical analyses (Zn, Al, Cr, Si, Cl, H) were performed in the Vernaison Analysis Center of CNRS. High-resolution MAS ^1H and ^{29}Si NMR spectra were obtained with a BRUKER MSL-300 spectrometer. Magic angle spinning was performed at a rate of 6000 Hz. ^1H NMR spectra were recorded with a $\pi/2$ impulsion delay of 10 μs and an acquisition time of 2 s. ^{29}Si NMR was realized with the CP-MAS technique and with a contact time of 40 ms and an acquisition time of 5 s. The chemical shifts were given in ppm in comparison with TMS taken as external reference. ^{27}Al NMR spectra were recorded

[†] Laboratoire de Physico-Chimie des Matériaux, URA CNRS 444.
[‡] LASMEA, URA CNRS 1793.
* To whom all correspondence should be addressed.
[⊗] Abstract published in *Advance ACS Abstracts,* March 1, 1996.

(1) Allmann, R. *Acta. Crystallogr.* **1968**, *B24*, 972.
(2) Miyata, S.; Okada, A. *Clays Clay Miner.* **1977**, *25*, 14.
(3) Depège, C.; Forano, C.; de Roy, A.; Besse, J. P. *Mol. Cryst. Liq. Cryst.* **1994**, *244*, 161−166.
(4) Boehm, H.; Steinle, J.; Vieweger, C. *Angew. Chem., Int. Ed. Engl.* **1977**, *16*, 265.
(5) Martin, K. J.; Pinnavaia, T. J. *J. Am. Chem. Soc.* **1986**, *108*, 541.
(6) Meyn, M.; Beneke, K.; Lagaly, G. *Inorg. Chem.* **1990**, *29*, 5201.
(7) Drezdzon, M. A. *Inorg. Chem.* **1988**, *27*, 4628−4632.
(8) Clearfield, A. *Chem. Rev.* **1988**, *88*, 125−148.
(9) Cavani, F.; Trifiro, F.; Vaccari, A. *Catal. Today* **1991**, *11*, 173−291.
(10) Mousty, C.; Therias, S.; Forano, C.; Besse, J. P. *J. Electroanal. Chem.* **1994**, *63*, 374.
(11) Moneyron, J. E.; de Roy, A.; Forano, C.; Besse, J. P. *Appl. Clay Sci.* **1995**, *10*, 163−175.
(12) Tagaya, H.; Sato, S.; Morioka, H.; Kadokawa, J. I.; Karasu, M.; Chiba, K. *Chem. Mater.* **1993**, *5*, 1431.

0897-4756/96/2808-0952$12.00/0

on a Bruker CXP-300 spectrometer (^{27}Al 78 MHz) at the magic angle spinning. The duration of a pulse was 1 s and the number of accumulations was 1500. The reference centered at 0 ppm was $Al(H_2O)_6^{3+}$ ion in aqueous solution.

Preparation. All the prepared LDH phases will be named following the abbreviated nomenclature $[Zn_R-M^{III}\text{-}X]_{prep}$ where R is the initial Zn^{2+}/M^{3+} ratio ($M^{3+} = Al^{3+}$ or Cr^{3+}) of the metallic salt reagent solution and X the intercalated anion. Prep stands for the preparation method: cop for coprecipitation at constant pH and exc for anionic exchange reaction.

Synthesis of Silicate Phases. *Preparation of Silicate Solution.* The silicate solution was prepared by dissolving 2 g of sodium metasilicate (Na_2SiO_3) in 200 mL of decarbonated water (0.08 M solution). The pH of this solution was 12. According to data concerning the solubility of SiO_2 versus pH,[13] the prepared silicate solution contained both $HSiO_3^-$ and SiO_3^{2-} species.

Precursor Synthesis. Exchange reactions were performed on the following precursor compounds: $[Zn_2-Cr-Cl]$, $[Zn_2-Al-Cl]$ and $[Zn_3-Al-Cl]$. These materials were prepared by the method of coprecipitation at constant pH following previous procedures.[14−16]

Practically, molar solutions of divalent and trivalent metals (in proportions to obtain the desired ratio *R*) were added at a constant flow (4 mL/h) in a flask containing 100 mL of distilled and deionized water. The LDH phases were precipitated at a pH of 4.7 for the Zn−Cr matrix and 9.0 for the Zn−Al one by a 1 M NaOH solution added using an automated titrator. The coprecipitation was carried out at room temperature under nitrogen atmosphere and with a vigorous magnetic stirring. The addition of the metallic salts solution was completed in 10 h, and the mixture was then left to react for 24 h. The LDH recovering was obtained by four successive washings using 250 mL of freshly decarbonated water and centrifugation cycles. The obtained precipitates were then dried at 30 °C under room relative humidity conditions (50−60% RH) during 24 h.

Anionic Exchange Reaction at pH = 12. The compounds to be exchanged were dissolved in the silicate solution (prepared as described before) at pH = 12, which then was refluxed at 100 °C during 24 h under continuous stirring. To minimize the problem of carbonation due to the basic pH, we have always used freshly prepared silicate solutions, previously subjected to nitrogen bubbling during 15 min. The LDHs were recovered using the same procedure as for coprecipitation.

The compounds obtained by exchange reaction at this pH are noted $[Zn_2-Al-SiO_4]_{exc.12}$ and $[Zn_3-Al-SiO_4]_{exc.12}$.

In the case of the $[Zn_2-Cr-Cl]$ precursor, no exchange at all was obtained. Both DRX and FTIR techniques confirmed the intercalation of carbonate anions. We have then tried to exchange the silicate anions on another precursor: $[Zn_2-Cr-NO_3]$. Indeed, the nitrate anion size is bigger than that of chloride, so the interlamellar distance increases which is likely to favor the silicate insertion. The $[Zn_2-Cr-NO_3]$ phase was prepared by an anionic exchange reaction on $[Zn_2-Cr-Cl]$ with a 1 M $NaNO_3$ solution for 12 h, under a nitrogen atmosphere. The exchange with silicate solution was carried out in the same operating conditions as before. The obtained compound is noted $[Zn_2-Cr-SiO_4]_{exc.12}$.

Anionic Exchange Reaction at pH = 9. In order to test the influence of pH on the obtaining of intercalated phases, we have exchanged the $[Zn_3-Al-Cl]_{cop}$ phase with a silicate solution at pH = 9. This was the value chosen by Schutz et al.[17] for the preparation of $[Mg_3-Al-HSi_2O_5]$. In this case, the compound to be exchanged was dissolved in a silicic acid solution. It is prepared by addition of a molar nitric acid solution to an aqueous suspension of sodium metasilicate prepared as described before. The obtained compound is noted $[Zn_3-Al-SiO_4]_{exc.9}$.

Table 1. Composition in Metallic Elements for the Different [Zn−Al] and [Zn−Cr] Synthesized Compounds

compound	Zn (%) ± 0.5%	Cr (%) ± 0.5%	Al (%) ± 0.5%	Si (%) ± 0.2%	Zn/M^{III}	Si/M^{III}
$[Zn_3-Al-Cl]_{cop}$	45.2		6.5		2.89	
$[Zn_2-Al-Cl]_{cop}$	39.4		8.3		1.98	
$[Zn_2-Cr-NO_3]_{exc}$	35.8	14.9			1.87	
$[Zn_3-Al-SiO_4]_{exc.12}$	45.3		6.4	7.6	2.95	1.15
$[Zn_2-Al-SiO_4]_{exc.12}$	39.8		7.9	11.5	2.08	1.40
$[Zn_3-Al-SiO_4]_{exc.9}$	43.2		5.4	13.2	3.29	2.35
$[Zn_3-Al-SiO_4]_{cop}$	44.6		6.2	7.6	2.98	1.21
$[Zn_2-Cr-SiO_4]_{exc.12}$	35.4	14.5		15.2	1.91	1.90

Direct Preparation by Coprecipitation. It is possible to insert the silicate anions directly during the reaction of formation of the hydroxylated sheets by the coprecipitation method. The reaction pH was imposed by the stability of the silicic acid solution. Then, it was not possible to work at pH less than 9 because of the formation of amorphous silica at lower values[18] with a very low solubility. So, the syntheses were carried out at pH = 9 from molar nitrate solutions of Zn, Al, or Cr with the following ratios: Zn/Al = 3 and Zn/Cr = 2. These solutions were progressively added to the silicic acid solution whose pH was maintained at a value of 9 by addition of 1 M NaOH solution. After an aging time of 24 h in the mother liquor at 90 °C, the precipitate was recovered by centrifugation, washed four times with decarbonated water, and then air-dried.

By this method, we have synthesized the $[Zn_3-Al-SiO_4]_{cop}$ compound. On the other hand, a crystallized $[Zn_2-Cr-SiO_4]_{cop}$ phase could not been obtained; this attempt was bound to fail because of the incompatibility of pH domains between the formation of the hydroxylated Zn−Cr matrix (pH = 4−5) and the silicate anions stability (pH > 9).

Results and Discussion

Characterization. *Chemical Analysis.* The Zn-, Al-, and Cr-weighted percentages were determined by atomic emission spectrometry with a plasma source. The Si contents were obtained by gravimetry of SiO_2.

The weighted concentrations for each compound are reported in Table 1, along with the Zn/M^{III} and Si/M^{III} ratios. We can see that the Zn/Al or Zn/Cr ratio is well maintained after the intercalation of silicate anions. Nevertheless, it is important to check if the results are compatible or not with the general formulae of hydrotalcite-like phases:

$$[M^{II}_{1-x}M^{III}_{x}(OH)_2]^{x+}[A^{m-}_{x/m}\cdot nH_2O]^{x-}$$

To have the neutrality of the charges, we need x/m silicate anions for one $[M^{II}_{1-x}M^{III}_{x}(OH)_2]^{x+}$ group, the Si/M^{III} ratio must then be equal to 1/*m* (*m* is the charge of the silicate anion). If we suppose that A^{m-} is $HSiO_3^-$, the Si/M^{III} ratio must be equal to 1. In the case of $[Zn_3-Al-SiO_4]_{exc.12}$, $[Zn_2-Al-SiO_4]_{exc.12}$, and $[Zn_3-Al-SiO_4]_{cop}$, the Si/Al ratio is lightly higher than 1; in the case of $[Zn_3-Al-SiO_4]_{exc.9}$ and $[Zn_2-Cr-SiO_4]_{exc.12}$, it is near 2. Then, it seems that the different synthesis methods do not lead to the same intercalated phases. But on the other hand, we cannot exclude the possibility of an adsorption of a part of silicate anions on the microcrystallites surface, the chemical analysis does not allow to distinguish the intercalated silicates and the adsorbed ones.

X-ray Diffraction. Precursors. Representative X-ray diffraction patterns of $[Zn_2-Cr-Cl]_{cop}$, $[Zn_2-Al-Cl]_{cop}$, and $[Zn_3-Al-Cl]_{cop}$ LDH phases are shown in Figure 1. They are characteristic of well-crystallized products

(13) Pourbaix, M. *Atlas d'Equilibres Electrochimiques*; Gautier-Villars & Cie, 1963.
(14) Reichle, W. T. *Solid State Ionics* **1986**, *22*, 135.
(15) Miyata, S. *Clays Clay Miner.* **1975**, *23*, 369.
(16) Miyata, S. *Clays Clay Miner.* **1980**, *28*, 50.
(17) Schutz, A.; Biloën, P. *J. Solid State Chem.* **1987**, *68*, 360.
(18) Pascal, P. *Nouveau Traité de Chimie Minérale*, Vol.VIII, Masson et Cie, 1965.

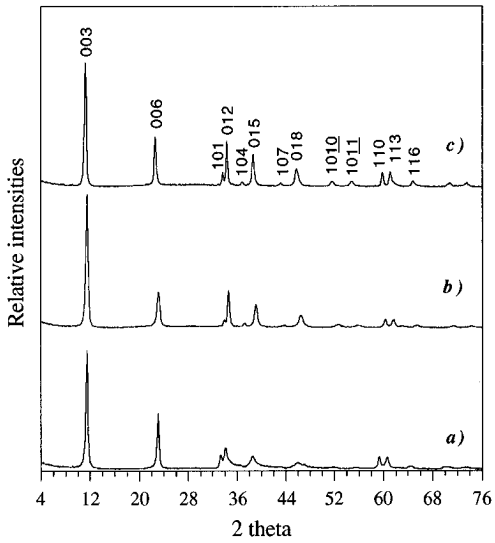

Figure 1. PXRD patterns of (a) $[Zn_2-Cr-Cl]$, (b) $[Zn_2-Al-Cl]$, and (c) $[Zn_3-Al-Cl]$ prepared by coprecipitation.

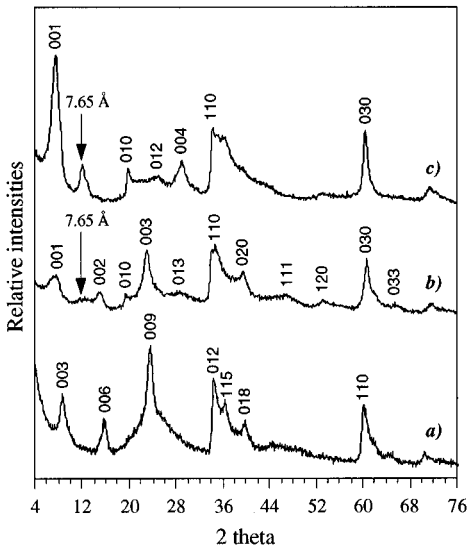

Figure 2. PXRD patterns of (a) $[Zn_2-Cr-SiO_4]$, (b) $[Zn_2-Al-SiO_4]$, and (c) $[Zn_3-Al-SiO_4]$ prepared by exchange reaction on chloride phases at pH = 12.0.

with a bidimensional structure, compounds which exhibit a $R\bar{3}$m symmetry and an hexagonal lattice.

Silicate Phases Exchanged at pH = 12. The PXRD patterns of $[Zn_3-Al-SiO_4]_{exc.12}$, $[Zn_2-Al-SiO_4]_{exc.12}$, and $[Zn_2-Cr-SiO_4]_{exc.12}$ LDHs are shown in Figure 2.

In the case of $[Zn_3-Al-SiO_4]_{exc.12}$, there is coexistence of two LDH phases: one with a short interlayer distance of 7.65 Å and a second major one with an interlayer distance of 12.45 Å. Such value indicates clearly the presence of silicate anions in the interlamellar space. Moreover, an analogous 12 Å LDH phase was reported by Schutz et al.[17] for the chemical composition $[Mg_3Al(OH)_8]^+[HSi_2O_5]^-$. Indexing of the diffraction lines has been carried out for an hexagonal symmetry with three different stacking sequences 3R, 2H, and 1H usually observed in the case of natural LDHs. Another indexing mode with a superstructure in the (*ab*) plane has also been envisaged. The results are presented in Table 2.

The description of the $[Zn_3-Al-SiO_4]_{exc.12}$ diffractogram in a rhombohedral symmetry (3*R*) is excluded by the presence of two diffraction lines centered at 4.65 and 3.69 Å which cannot be indexed. The same phenomenon is observed with the use of 1H (one sheet) or 2H (two sheets) stacking sequences. On the other hand, calculations based on a superstructure parallel to the sheet planes gives a much better indexing. So, the structural indexing of this phase can be obtained in a 1H hexagonal stacking mode with a superstructure in the (*ab*) plane leading to the following cell parameters:

$$a = \sqrt{3}a_{\text{brucite}} = 5.305 \text{ Å}$$

$$c = d_{\text{intermellar}} = 12.45 \text{ Å}$$

This superstructure arises here from a particular ordering of the anionic entities in the interlayer domain. Such a superstructure has already been observed in the case of the intercalation of SO_4^{2-} anions in [Zn−Cr] LDHs.[19,20] However, this hypothesis does not allow us to explain the diffraction line at 7.65 Å. This could be a (003) reflection of a $[Zn_3-Al-CO_3]$ phase but a FTIR study excludes the presence of carbonate anions. So, this phase probably corresponds to a contracted $[Zn_3-Al-SiO_4]$ secondary phase.

The PXRD pattern of $[Zn_2-Al-SiO_4]_{exc.12}$ is relatively similar to that of $[Zn_3-Al-SiO_4]_{exc.12}$ with two phases at the same distances (12.45 and 7.65 Å), but we can notice an important decrease in the intensity of these two diffraction lines. It is probably due to the decrease in Zn^{2+}/Al^{3+} metallic ratio which involves an increase in the concentration of the intercalated anions.

For the $[Zn_2-Cr-SiO_4]_{exc.12}$ system, the exchange reaction leads to a unique crystallized LDH phase with a basal spacing of 11.89 Å. The identification of the diffraction lines has been performed in a 3*R* stacking sequence as for the nitrate precursor.

Silicate Phases at pH = 9. The PXRD pattern of $[Zn_3-Al-SiO_4]_{cop}$, and $[Zn_3-Al-SiO_4]_{exc.9}$ LDHs are shown in Figure 3. The coprecipitation method leads to a very poorly crystallized hydrotalcite-like phase, with an interlamellar spacing of 7.65 Å. No stacking sequence can be determined.

The exchanged phase at the same pH is better crystallized with also a secondary amorphous phase. The diffraction lines can be indexed in the $R\bar{3}m$ space group with a basal spacing of 7.65 Å.

FTIR Spectroscopy. $[Zn_2-Cr-SiO_4]_{exc.12}$. The FTIR spectra of $[Zn_2-Cr-SiO_4]_{exc.12}$ and $[Zn_2-Cr-Cl]_{cop}$ precursor are reported in Figure 4.

For the intercalated phase, we observe a broad disymmetric band in the 3000−4000 cm^{-1} range, which results from the superposition of two bands: the ν_{OH} vibration band of the brucitic sheets centered at 3422 cm^{-1}; the ν_{OH} vibration band of water molecules centered at 3100 cm^{-1}.

The high intensity of this band supposes an important hydration of the compound. Among all vibration bands, we can also identify the δ_{H-O-H} vibration band at 1640 cm^{-1} and the vibration bands of the hydroxylated sheets at 400, 520, and 585 cm^{-1} (these bands are identical with those of $[Zn_2-Cr-Cl]_{cop}$, intercalation of silicate species does not affect the brucitic sheets), and the $\nu_3(CO_3^{2-})$ vibration band at 1360 cm^{-1} due to the

(19) Ennadi, A.; Khaldi, M.; de Roy, A.; Besse, J. P. *Mol. Cryst. Liq. Cryst.* **1994**, *244*, 373−378.
(20) Khaldi, M. Ph.D. Thesis, Université Blaise Pascal, Clermont II, France, 1995.

Table 2. Comparison of *d* Spacings Observed for the $[Zn_3-Al-SiO_4]_{exc.12}$ Phase with Those Calculated for Stacking Sequences Corresponding to One Sheet, Two Sheets, or Three Sheets or to a Superstructure

compound $[Zn_3-Al-SiO_4]$ prepared by anionic exchange reaction (pH 12)	stacking sequence (1H) $a = 3.063$ Å $c = 12.45$ Å		(2H) $a = 3.063$ Å $c = 24.91$ Å		(3R) $a = 3.063$ Å $c = 37.36$ Å		superstructure $a = \sqrt{3}a_{hydro}$ $c = 12.45$ Å	
d_{obs} (Å)	d_{calc} (Å)	*hkl*	d_{calc} (Å)	*hkl*	d_{calc} (Å)	*hkl*	d_{calc} (Å)	*hkl*
12.455	12.455	001	12.455	002	12.455	003	12.455	001
7.687	?	?	?	?	?	?	?	?
	6.227	002	6.227	004	6.228	006	6.228	002
			4.983	005				
4.565							4.594	010
	4.151	003	4.152	006	4.152	009	4.152	003
3.698							3.697	012
			3.559	007				
3.116	3.114	004	3.114	008	3.114	0012	3.114	004
	2.652	010	2.652	010	2.646	101	2.652	110
2.636			2.638	011	2.626	012		
1.531	1.531	110	1.5315	110	1.531	110	1.531	030
1.319	1.319	021	1.319	022	1.3131	024	1.319	220

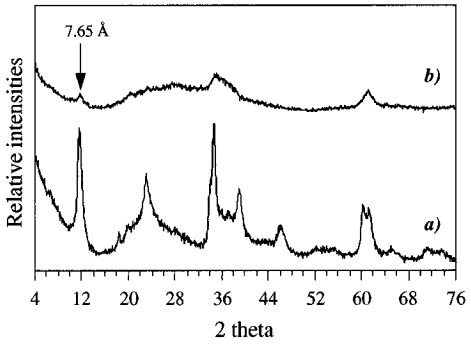

Figure 3. PXRD patterns of $[Zn_3-Al-SiO_4]$ prepared (a) by exchange reaction on chloride phase at pH = 9.0 and (b) by coprecipitation.

contamination of the phase by carbonate anions during the synthesis.

The presence of silicate species in the Zn−Cr matrix is shown by the following characteristic vibrations: asymmetric ν_3(Si−O) at 1000 cm^{-1};[17] symmetric ν_1(Si−O) at 800 cm^{-1} (reported at 819 cm^{-1} for SiO_4^{4-});[21] δ(Si−O−Si) at 1200 cm^{-1}.[17,22]

The ν_1(Si−O) vibration band at 800 cm^{-1} accounts for a lowering of symmetry of the tetracoordinated silicium atom in comparison with the perfect SiO_4^{4-} tetrahedron.[21] This lowering of symmetry can be attributed to the condensation of SiO_4 polyhedron, condensation confirmed by the existence of the δ(Si−O−Si) vibration band. The occurrence of the band at about 1200 cm^{-1} is characteristic of the 180° Si−O−Si stretching vibration found in an inverted connecting frame between two straight-linked SiO_4 tetrahedral groups (Figure 5).[17]

$[Zn_3-Al-SiO_4]_{exc.12}$ and $[Zn_3-Al-SiO_4]_{cop}$. The FTIR spectra of $[Zn_3-Al-SiO_4]_{exc.12}$, $[Zn_3-Al-SiO_4]_{cop}$, and $[Zn_3-Al-Cl]_{cop}$ precursor are shown in Figure 6.

In the case of $[Zn_3-Al-SiO_4]_{exc.12}$, several bands are observed:

(i) A broad band around 3000 cm^{-1} (its intensity is lower than that observed for $[Zn_2-Cr-SiO_4]_{exc.12}$, which accounts for a lower concentration in OH groups and H_2O molecules). This band comes from the contribution of three species: ν_{OH} of brucitic sheets at 3460 cm^{-1}; ν_{OH} of water molecules at about 3100−3160 cm^{-1}; ν_{OH} of free OH functions at 3630 cm^{-1}. It can be attributed to lamellar metallic hydroxides,[23,24] $M(OH)_2$ or free silanol groups (a band at 3600 cm^{-1} is observed in the case of $H_2Si_{14}O_{29}\cdot 5.4H_2O$).[25]

(ii) Vibration bands of the hydroxylated sheets at 435 and 647 cm^{-1}.

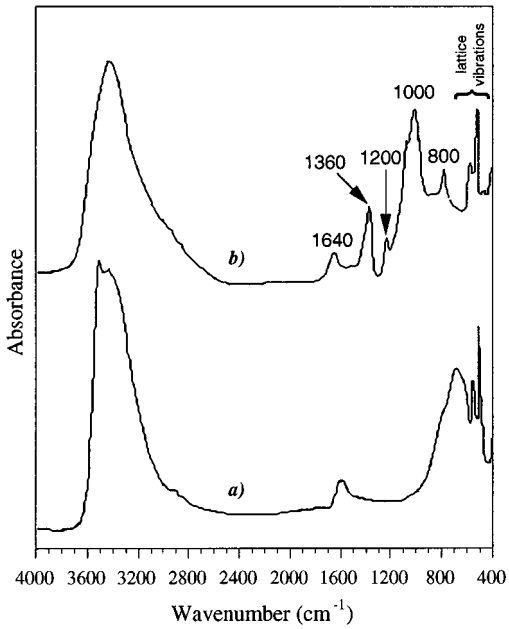

Figure 4. FTIR spectra of (a) $[Zn_2-Cr-Cl]_{cop}$ and (b) $[Zn_2-Cr-SiO_4]_{exc.12}$.

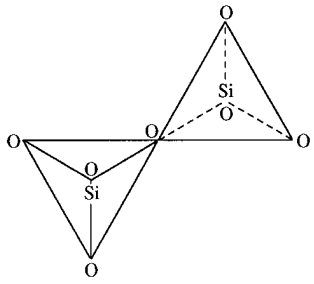

Figure 5. Condensation mode of SiO_4 unit in $[Zn-Cr-SiO_4]$ compounds.

(21) Nakamoto, K. *Infrared and Raman spectra of inorganic and coordination compounds;* John Wiley and Sons: New York, 1986.
(22) Clay Mineralogy. In *Spectroscopic and Chemical Determinative Methods*; Wilson, M. J., Ed.; Chapman & Hall: London, 1994.
(23) Brindley, G. W.; Kao, C. C. *Phys. Chem. Miner.* **1984**, *10*, 187.
(24) Dawson, P.; Hardfeild, C. D.; Wilkinson, G. R. *J. Chem. Phys. Solids* **1973**, *34*, 1217.
(25) Pinnavaia, T. J.; Johnson, I. D. *J. Solid State Chem.* **1986**, *63*, 118.

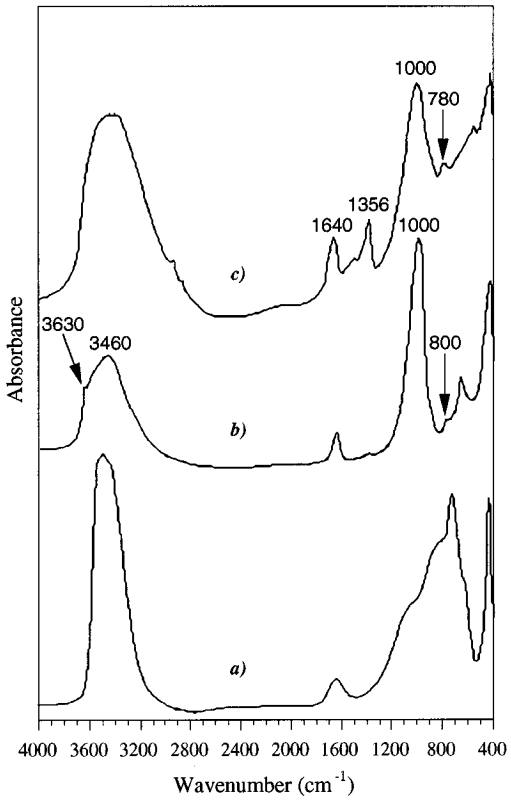

Figure 6. FTIR spectra of (a) $[Zn_3-Al-Cl]_{cop}$, (b) $[Zn_3-Al-SiO_4]_{exc.12}$, and (c) $[Zn_3-Al-SiO_4]_{cop}$.

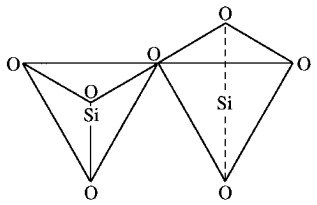

Figure 7. Condensation mode of SiO_4 unit in $[Zn-Al-SiO_4]$ compounds.

(iii) ν_1(Si−O) at 800 cm^{-1}.

(iv) ν_3(Si−O) at 1000 cm^{-1} (of great intensity).

On the other hand, the absence of δ(Si−O−Si) vibration band at 1200 cm^{-1} seems to indicate a different mode of silicate condensation, with a SiO_4 tetrahedron of the same orientation (Figure 7). The Si−O−Si angle is then near 140°. We can also note an absence of contamination by carbonate anions.

The FTIR spectrum of the coprecipitated phase $[Zn_3-Al-SiO_4]_{cop}$ presents small differences with the latter compound: (i) the hydration state is higher in this phase and no fine band corresponding to free OH functions is observed (the two phases seem to be of a different nature); (ii) the lattice vibrations of the host structure are badly resolved, which confirms a strong modification in the brucitic sheets already shown by X-ray diffraction; (iii) the vibration bands of intercalated silicate species are identified at 1000 cm^{-1} (ν_3(Si−O)) and at 780 cm^{-1} (ν_1(Si−O)); (iv) the compound is contaminated by CO_3^{2-} anions ($\nu_3(CO_3^{2-})$ at 1356 cm^{-1}).

Nuclear Magnetic Resonance. ^{1}H, ^{29}Si, and ^{27}Al solid-state NMR experiments have been carried out in addition to FTIR analysis to identify the silicate nanostructure in the [Zn−Al] interlayers.

^{1}H NMR. ^{1}H NMR spectra of chloride precursors (Figure 8a) show the existence of broad bands non-

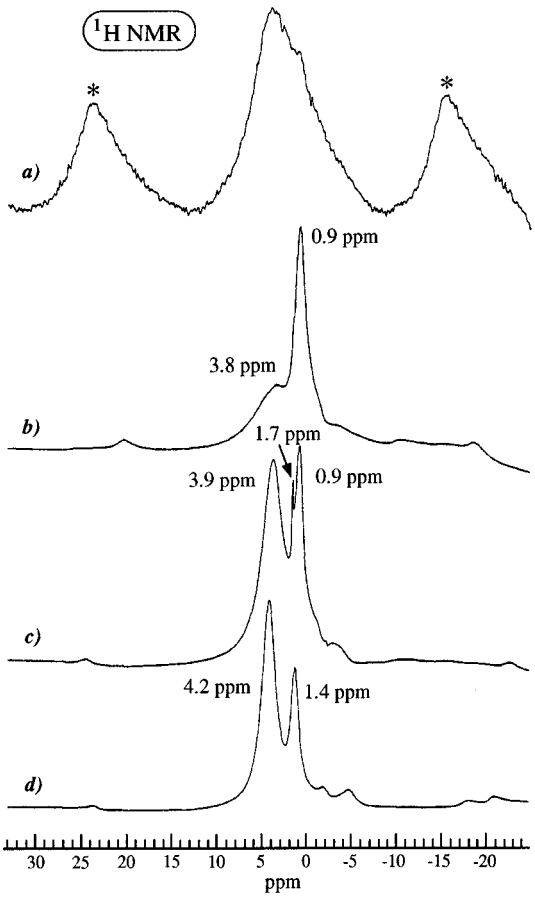

Figure 8. ^{1}H MAS NMR spectra of (a) $[Zn_3-Al-Cl]_{cop.}$ and of $[Zn_3-Al-SiO_4]_{exc.12}$, (b) calcined at 100 °C, (c) heated in situ at 100 °C, and (d) as prepared (asterisks spinning sidebands).

resolved and characteristic of OH and H_2O.[26] Strong ^{1}H−^{1}H dipolar interactions due to OH and H_2O protons lead to about 3 kHz large peaks (30 kHz line width without spinning), the diffusion properties increasing the number of interactions between OH and H_2O species. The layered double hydroxides are known for their property of good protonic conductors.[27] This conductivity is due to the high mobility of the protons of M−O−H and H_2O species in interlamellar domains, involved in the $M-OH + H_2O \rightarrow M-O^- + H_3O^+$ proton transfer. The protonic diffusion in such lamellar structures is generally favored by strongly polarizing anions.

$[Zn_3-Al-SiO_4]_{exc.12}$ intercalated phases present very different ^{1}H NMR spectra. These spectra show well-resolved multiplets with narrow width (400 and 530 Hz), centered at chemical shifts equal to respectively 1.4 ppm and 4.2 ppm (Figure 8d). The same spectra are observed for the $[Zn_3-Al-SiO_4]$ coprecipitated phases.

It is worth noting that a high resolution is obtained for these compounds in ^{1}H NMR which is rarely the case for solids because of strong dipolar interactions. The high resolution of these spectra can be compared to those of some hydrated minerals studied by Yesinowski et al.[28] and more particularly to the spectrum of hydroxyapatite $Ca_5(PO_4)_3OH$ for which hydroxyls, water molecules of structure, or adsorbed are identified. Some

(26) Dupuis, J.; Battut, J. P.; Fawal, Z.; Hajjimohamad, H.; de Roy, A.; Besse, J.P. *Solid State Ionics* **1990**, *42*, 251.
(27) de Roy, A.; Besse, J. P. *Solid State Ionics* **1989**, *35*, 35−43.
(28) Yesinowski, J. P.; Eckert, H. *J. Am. Chem. Soc.* **1987**, *109*, 6274.

Table 3. ^{1}H NMR Chemical Shifts of Some Mineral Compounds Compared with Those of Our Phases

compound	M_{Oh}−OH	M_{Td}−OH	H_2O (structure)	H_2O (adsorbed)	ref
$Mg_3Si_4O_{10}(OH)_2$ (talc)	1.1				30
$Ca_2Mg_5Si_8O_{22}(OH)_2$	0.7				31
$Al_2Si_4O_{10}(OH)_2$		2.3			32
$CaSO_4{\cdot}2H_2O$			5.3		33
$NaAlSi_2O_6{\cdot}H_2O$			3.1		34
SiO_2 (quartz)				4.8	35
(Na,K)$AlSiO_4$ (nephelite)				4.6	36, 37
$[Zn_3-Al-SiO_4]_{exc.12}$ heated in situ or in oven at 100 °C	0.9	1.7		3.9	this work
$[Zn_3-Al-SiO_4]_{exc.12}$	1.4			4.2	this work
$Ca_5(PO_4)_3OH$		0.2		5.6	28

examples given by Yesinowski[29] and our samples are reported in Table 3.

The evolution of the spectra of $[Zn_3-Al-SiO_4]_{exc.12}$ after thermal treatment in an oven at 100 °C (Figure 8b) shows a decrease in the intensity of the band centered at 4.2 ppm which corresponds to the ^{1}H nuclei of adsorbed water molecules (Table 3). The second band centered at 1.4 ppm corresponds to OH groups of the brucitic sheets. A moderate heating at 100 °C leads to a shift of the bands toward low values (respectively 3.9 and 0.9 ppm). An additional band at 1.7 ppm appears after these thermal treatments, very clearly in the case of an in situ heating (Figure 8c) and in the form of a shoulder for a heating in oven (Figure 8b). This value could correspond to the chemical shift of Si−OH groups observed at low field in comparison with the metallic hydroxides.[38]

The observed bands of narrow width are in contradiction with the presence of strong hydrogen interactions between several protonated species usually observed for LDHs protonic conductors. The existence of several species characterized by fine bands can be explained by weak ^{1}H−^{1}H dipolar interactions. These protonated species are then isolated, and this hypothesis excludes the presence of water molecules in interlamellar domains, in contact with OH groups of brucitic sheets. Moreover, the presence of free OH functions has been shown by infrared spectroscopy. The low water content, compared to other LDH phases, has also been confirmed by FTIR and thermogravimetric analysis. This important structural difference compared to other hydrotalcite-like phases can be explained only by the polycondensation of silicate species between the $[Zn_3Al(OH)_8]^+$ sheets, in agreement with X-ray diffraction and ^{29}Si NMR.

^{29}Si NMR. Nuclear magnetic resonance is a characterization technique particularly suitable for the structural study of near environment of ^{29}Si nuclei. Notably, it is very sensitive to the condensation degree x of $Si(OSi)_x(OH)_{4-x}$ species and to the substitution degree y of the second Si neighbors by another element, $Si(OSi)_{x-y}(OM)_y(OH)_{4-x}$ (where M = Al, Ga, etc.) and is very used for the structural characterization of silicic acids, clays, and zeolites.

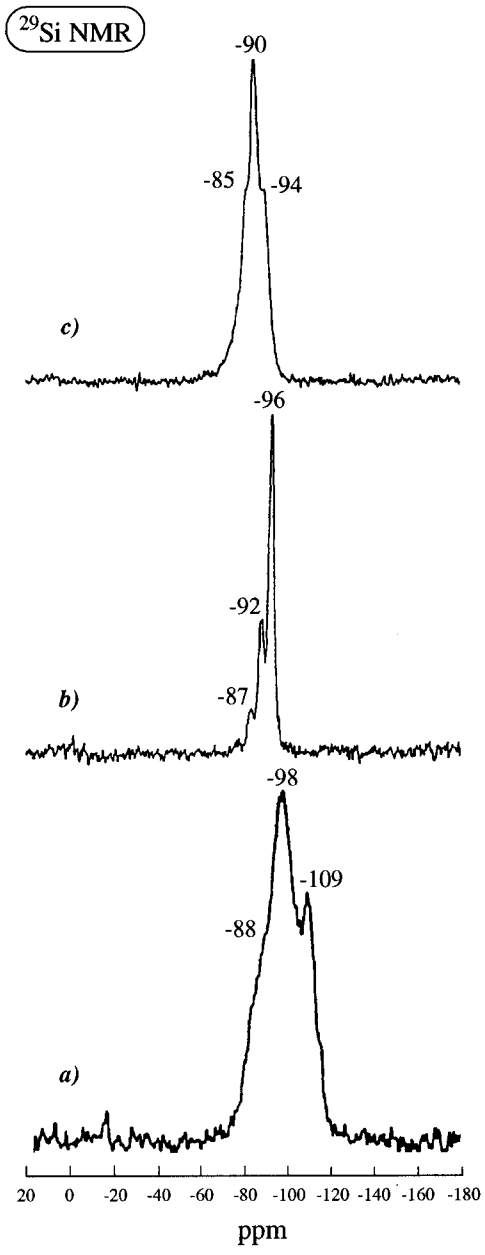

Figure 9. ^{29}Si CP-MAS NMR spectra of (a) $[Zn_3-Al-SiO_4]_{exc.9}$, (b) $[Zn_3-Al-SiO_4]_{exc.12}$, and (c) $[Zn_3-Al-SiO_4]_{cop}$.

In Figure 9 are reported the ^{29}Si CP-MAS NMR spectra of $[Zn_3-Al-SiO_4]$ phases obtained by either coprecipitation or anionic exchange reaction at pH 9 and 12.

The spectra obtained for $[Zn_3-Al-SiO_4]_{exc.9}$ show a series of overlapping peaks pointed at −109, −98, and −88 ppm. These peaks are shifted by values of about 10 ppm (Figure 9a). In the case of silica and lamellar silicates, this shift corresponds to different substitution

(29) Yesinowski, J. P.; Eckert, H.; Rossman, R. G. *J. Am. Chem. Soc.* **1988**, *110*, 1367.
(30) Perdikatsis, B.; Burtzlaff, H. Z. *Kristallogr.* **1981**, *156*, 177.
(31) Hawthorne, F. C.; Grundy, H. D. *Can. Miner.* **1976**, *14*, 334.
(32) Hendricks, S. B. Z. *Kristrallogr.* **1938**, *99*, 264.
(33) Cole, W. F.; Lancucki, C. J. *Acta. Crystallogr.* **1974**, *B30*, 921.
(34) Mazzi, F.; Calli, E. *Am. Miner.* **1978**, *63*, 448.
(35) Legage, Y.; Donny, G. *Acta. Crystallogr.* **1970**, *B32*, 2456.
(36) Dollase, W. A. Z. *Kristallogr.* **1970**, *132*, 45.
(37) Foreman, N.; Peacor, D. R. Z. *Kristrallogr.* **1970**, *132*, 217.
(38) Legrand, A. P.; Hommel, H.; Taibi, H.; Miquel, J. L.; Tougne, P. *Colloids Surf.* **1990**, *4*, 391.

Table 4. ^{29}Si NMR Chemical Shifts of Some Mineral Compounds Compared with Those of Our Phases

compounds	$Si(Si_3)$	$Si(Si_2Al)$	$Si(SiAl_2)$	$Si(Al_3)$	Al_{tet}	Al_{oct}	ref
$NaHSi_2O_5 \cdot 3H_2O$	−101						25
talc	−97						40
kaolinite	−92						40
margarite				−73	+71	+2	40
phlogopite P8	−91	−86	−82		+63.5	+6	40
vermiculite	−92	−88	−83.5		+62.5	+5	40
$[Mg_3-Al-HSi_2O_5]$	−104					+9.3	17
$[Zn_3-Al-SiO_4]_{cop}$		−94; −90; −85			+54; +67	+12.5	this work
$[Zn_3-Al-SiO_4]_{exc.12}$		−96; −92; −87			?	?	this work
$[Zn_3-Al-Cl]_{cop}$						+13.5	this work

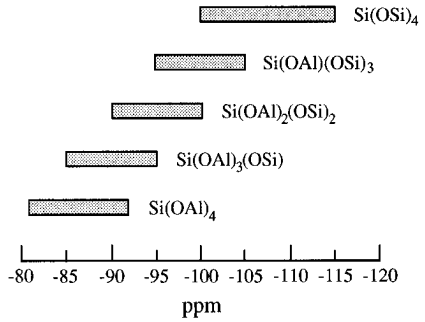

Figure 10. ^{29}Si chemical shifts for different $Si(OSi)_{4-y}(OAl)_y$ environments in zeolites.

rates x of hydroxyl group (−OH) by siloxane group (−OSi) around a tetrahedral Si central atom. Each peak represents the signal of a ^{29}Si nucleus with a $Si(OSi)_x(OH)_{4-x}$ structure. We find here the classical spectrum of amorphous silica with three peaks pointed at −109.3, −99.8 and −90.6 ppm[39] corresponding respectively to Si atom of $Si(OSi)_2(OH)_2$, $Si(OSi)_3(OH)$ and $Si(OSi)_4$ species.

The ^{29}Si NMR spectra of $[Zn_3-Al-SiO_4]_{exc.12}$ (Figure 9b) and $[Zn_3-Al-SiO_4]_{cop}$ (Figure 9c) are well-resolved with three very fine peaks pointed at respectively −96, −92, and −87 ppm and −94, −90, and −85 ppm.

These NMR chemical shift values are similar to those of ^{29}Si in phyllosilicate minerals (like talc, kaolinite, vermiculite, etc.)[40,41] where SiO_4 polyhedra polymerize by corner sharing into hexagonal layers which condense onto brucite-like or gibsite-like octahedral layers in a 1:1 or 2:1 manner (Table 4). We can conclude that a similar layered polymerization of SiO_4^{4-} has occurred in our phases in which the silicon environment is either of the type $Si(OSi)_{3-y}(OM)_y(OH)$ or $Si(OSi)_{3-y}(OM)_y(OM')$ with M = Al and M′ in an octahedral site. This distribution of composition for tridimensional aluminosilicates or zeolites leads to observe chemical shifts toward less negative values as the aluminum content increases in the coordination polyhedra (Figure 10).[42]

In the case of LDH phases with interlamellar distances respectively equal to 7.5 and 12.5 Å, the variation of intensity of the three peaks should then correspond to a different substitution rate for the two phases. These results seem to confirm a structural model very close to that of cationic clays.

^{27}Al NMR. ^{27}Al NMR experiments have been realized only on the $[Zn_3-Al-SiO_4]$ coprecipitated phase (Figure 11) and confirm the diffusion of Al^{3+} ions from the brucitic layers to the silicate layers already shown by

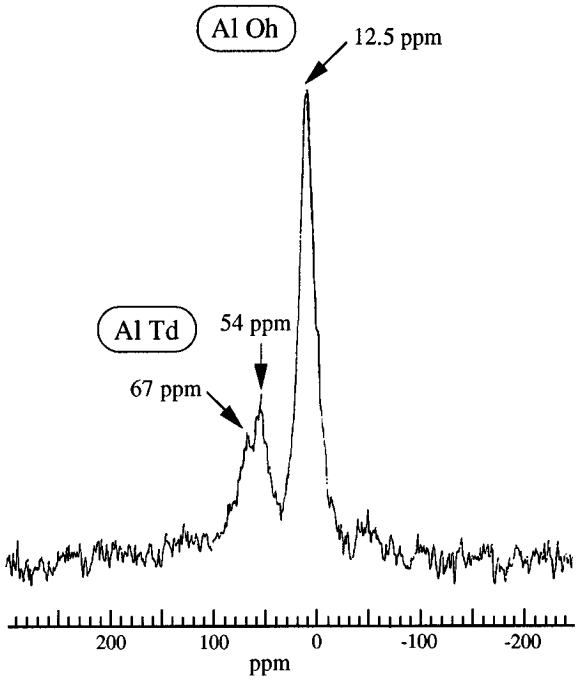

Figure 11. ^{27}Al CP-MAS NMR spectra of $[Zn_3-Al-SiO_4]_{cop}$.

^{29}Si NMR with the existence of $Si(OSi)_{3-x}(OAl)_x(OM)$ species. Indeed, both tetrahedral (δ = +54 ppm) and octahedral (δ = +12.5 ppm) environments for Al^{3+} ions are identified in the NMR spectra. This Al transfer must create vacancies in the brucitic layer and important charge-balance changes in the new structure with a decrease in the positive charge of the brucite-like layer and an increase in the charge of the silicate layer. Structural and chemical analogy between $[Zn-Al-SiO_4]$ and $[Zn-Cr-SiO_4]$ let us assume that polymerization of tetrahedral silicate layers also occurs in $[Zn-Cr-SiO_4]$.

Seefeld et al.[43] have also observed the formation of Al−O−Si bonds in [Mg−Al] LDHs. They have shown by NMR spectroscopy that up to 25% of the originally octahedrally coordinated Al was transformed into tetrahedrally coordinated Al.

Pillaring of Silicate Sheets On Layered Double Hydroxides. *$[Zn-Cr-SiO_4]$ Phases.* The evolution of the basal spacings of $[Zn_2-Cr-Cl]$ and $[Zn_2-Cr-SiO_4]_{exc.12}$ phases versus temperature is reported in Figure 12.

For the chloride precursor, the evolution of the d parameter is typical of a dehydration process with a decrease from 7.72 to 7.34 Å when the temperature

(39) Marciel, G. E.; Sindorf, D. W. *J. Am. Chem. Soc.* **1980**, *102*, 7607.
(40) Kinsey, R. A.; Kirkpatrick, R. J.; Hower, J.; Smith, K. A.; Oldfield, E. *Am. Miner.* **1985**, *70*, 537.
(41) Sanz, J.; Serratosa, J. M. *J. Am. Chem. Soc.* **1984**, *106*, 4790.
(42) Klinowski, J. *Solid State Ionics* **1985**, *16*, 3.
(43) Seefeld, V.; Gessner, W.; Schülke, U. *Symposium on Synthesis of Zeolites, Layered Compounds and Other Microporous Solids*, Anaheim, CA, April 2−7; American Chemical Society: Washington DC, 1995, pp 314−316.

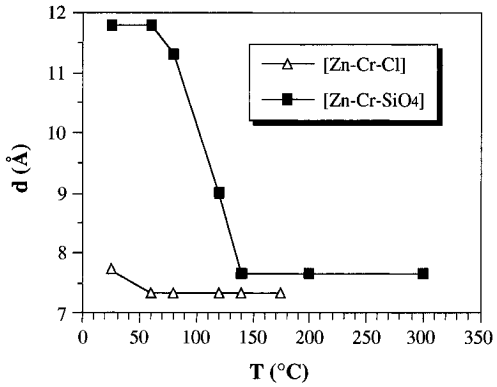

Figure 12. Evolution of the basal spacings of $[Zn_2-Cr-Cl]_{cop}$ and $[Zn_2-Cr-SiO_4]_{exc.12}$ with the temperature of calcination.

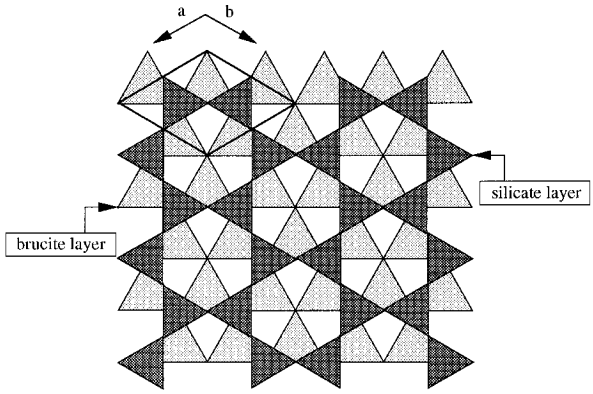

Figure 13. Hexagonal symmetry retention under brucite and silicate layers condensation.

increases from 25 to 180 °C. It corresponds to the elimination of part of water molecules in the interlamellar space.

For the silicate phase, the behavior versus temperature is totally different. Indeed, we observe a strong interlayer spacing contraction from 11.90 Å at 25 °C to 7.65 Å at 140 °C. This low value is maintained until 300 °C. Short basal spacings of 7.65 Å cannot account for free silicate layers in interlayer domains but must arise from a condensation process of silanol groups and metallic hydroxyls:

$$M-OH + Si-OH \rightarrow M-O-Si + H_2O$$

This condensation process onto brucitic layers yields to the formation of grafted tetrahedral−octahedral layers with the formation of new Si−O−M bonds and is rendered possible by compatible hexagonal symmetry of the two layers which possess condensable OH groups (Figure 13) and by the charge density of the layers which allows a packing based on a Metal/Si ratio equal to $^3/_2$. Such pillaring processes have already been demonstrated in [Cu−Cr] and [Zn−Cr] LDHs pillared by chromate or sulfate anions.[3,19,20,44]

The removal of intrinsic water molecules and the OH condensation are confirmed by a strong irreversible decrease in the ν_{O-H} vibration band intensity on the FTIR spectra (Figure 14). The thermal grafting process involves a deep change in the environments of both SiO_4 units and intralayer metallic cations. We can also observe a shift of the SiO_4 stretching bands toward the higher energies (from 1000 to 1100 cm^{-1}) and the

(44) El Malki, K.; de Roy, A.; Besse, J. P. *Eur. J. Solid State Inorg. Chem.* **1989**, *26*, 339.

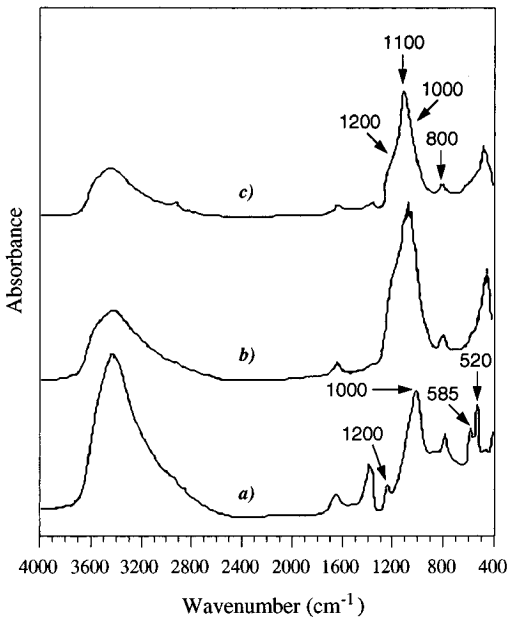

Figure 14. FTIR spectra of $[Zn_2-Cr-SiO_4]_{exc.12}$ at (a) 25 °C, (b) 80 °C, and (c) 140 °C.

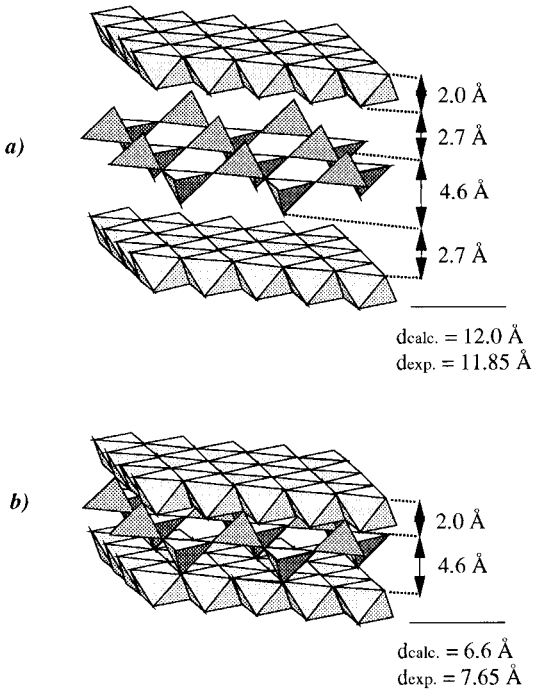

Figure 15. Structural model for $[Zn-Cr-SiO_4]$ compounds (a) before grafting and (b) after grafting.

disappearance of the two typical lattice bands of the brucitic layer (520 and 585 cm^{-1}).

All these results indicate that the SiO_4 units polymerize in the LDH interlamellar domains as inverted tetrahedral layers and that under mild calcinations these layers undergo an uniform grafting on the LDH brucitic layers resulting in new tridimensional structures ideally represented in Figure 15.

To confirm this hypothesis, the compounds previously calcined at 140 °C have been dissolved in a molar solution of sodium nitrate or sulfate. After a few hours, the precipitate is centrifuged, dried at room temperature, and then analyzed by the X-ray diffraction technique. No modification of the interlayer spacing is observed: its value remains near 7.65 Å. The same treatment has been applied to the non calcined $[Zn_2-$

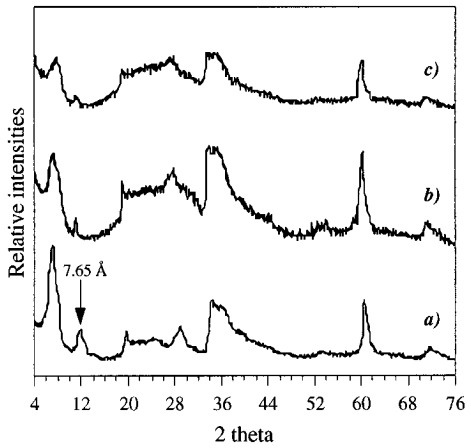

Figure 16. PXRD patterns of $[Zn_3-Al-SiO_4]_{exc.12}$ at (a) 25 °C, (b) 200 °C, and (c) 300°C.

$Cr-SiO_4]_{exc.12}$ phase. The X-ray diffractogram shows clearly that no exchange has occurred, the interlamellar distance remains at a value of 11.90 Å. These results can only be explained by the existence of a condensed silicate sheet in the interlayer domain.

[Zn−Al−SiO₄] Phases. For the $[Zn_3-Al-SiO_4]_{exc.12}$ compounds, no change in the interlayer spacing is observed under moderate heating, both 12.45 and 7.65 Å expanded lamellar phases remain noncontracted as shown by X-ray diffraction (Figure 16). No major dehydroxylation is observed on thermograms, and the grafting process of silicate layers onto octahedral double hydroxide layers has already occurred during the preparation, probably induced by the transfer of part of the Al^{3+} in tetrahedral layers. Moreover, the chemical analysis leads to an overall metal cation to silicon ratio not far from 4:1, which would correspond for a pure nanocomposite phase to one tetrahedral layer for two octahedral layers. Assumptions made only on interlayer distances can be proposed. Consequently, the new lamellar structure with a 12.45 Å basal spacing should result from an interstratification of brucite layers and 1:1 kaolinite-like layers (Figure 17). An analogous behavior is observed in chlorite, described as an interstratified mica/brucite mineral. On the other hand, the 7.65 Å phase could correspond to a structure with a simple tetrahedral/octahedral layers condensation, like that for serpentine 1:1 (d = 7.2 Å, Figure 18b). These structural models can also be applied to the $[Zn_2-Al-SiO_4]_{exc.12}$ phases.

The stability in temperature of these two phases (no modification of interlayer spacings) excludes the possibility of a supplementary condensation between the sheets, which is in good agreement with the proposed model.

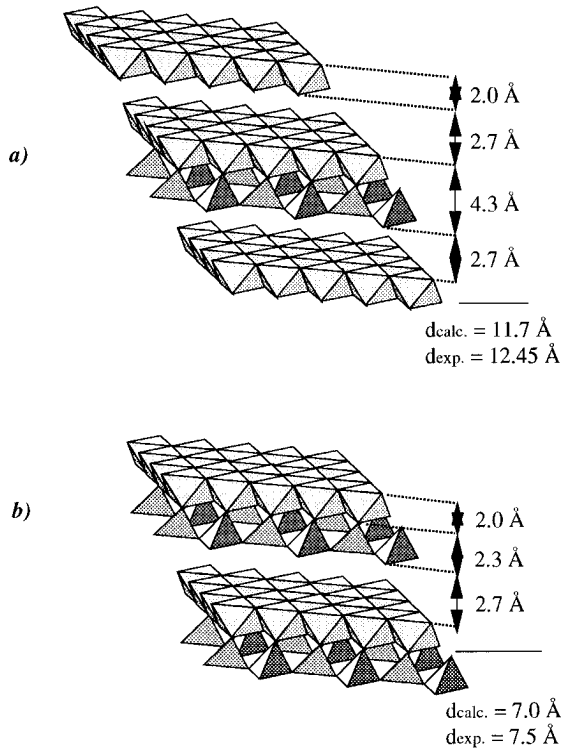

Figure 17. New interlayered LDH silicate phases in the case of $[Zn-Al-SiO_4]$ compounds.

Conclusion

These results provide evidence that the LDH interlayer domains can act as nanoreactors for the polymerization of inorganic oxo-anions. The obtaining of tetrahedral silicate sheets via the polymerization of SiO_4 polyhedra results in new interstratified phases, never prepared before, which easily undergo layer-to-layer condensation reactions, resulting in clay mineral structure like compounds. This appears as a promising synthetic approach to prepare, via a chimie douce route, new synthetic clays with tunable metallic cations composition. Expected new structural and chemical properties would result in interesting catalytic applications. Coating of silica crystallite support by LDH monolayers should normally be obtained in a similar way; this would be suitable to obtain nanocomposite materials based on LDH with improved surface properties.

Acknowledgment. We thank Professor Hélène Zanni (ESCPI Paris) for her contribution in the ^{27}Al NMR study.

CM950533K